INTERNATIONAL JOURNAL OF
COASTAL, OFFSHORE&ENVIRONMENTAL ENGINEERING IJCOE Vol.11/No. 2/Spring 2026 (1-11)

Available online at: www. Ijcoe.org

Experimental and numerical study of Scour beneath two Pipelines in tandem Due to Tidal Currents

Darioush Hosseini [1], Habib Hakimzadeh[2*]

[1] *Phd student, Faculty of Civil Engineering,Sahand University of Technology, Tabriz;d_hosseini@sut.ac.ir*
[2] *Professor, Faculty of Civil Engineering, Sahand University of Technology, Tabriz; hakimzadeh@sut.ac.ir*

ARTICLE INFO

Article History:
Received 11 Sep2025
Accepted 12 Feb 2025

Keywords:
Submarine Pipes
Tide
Sediment Transport
Laboratory Tests
Numerical Model

ABSTRACT

In industrial applications, multiple parallel pipelines are utilized to connect offshore platforms to coastal facilities. This configuration ensures uninterrupted operation of the coastal facilities in the event of damage to any individual pipeline. The flow and scour patterns around each pipeline are influenced by the factors such as the number of pipelines and their spacing from one to another. In this study, the impact of tidal currents on scouring beneath two identical pipelines placed in a tandem arrangement investigated using both experimental and numerical models. For this purpose, first, the hydrodynamic and sediment transport models based on Flow-3D are used to numerically simulate the local scour around the two tandem pipelines due to bidirectional tidal currents. Then, two series of experiments are carried out for the steady state and bidirectional flow conditions. The experimental results show that for tandem pipelines scour in clear water condition, the maximum scour depths under steady state flow condition exceeds than that caused by bidirectional flow. Further, the scour holes are highly dependent on the bidirectional flow velocity and tidal period as well as the gap between two pipes. When the gap between pipes is equal to one pipe diameter, the scouring depth is lower compared to closely conducted pipes. For this case, each pipe has a unique scour hole with limited dimensions. Finally, the numerical results have been compared with the corresponding experimental data and a relatively good agreement was achieved between them.

1. Introduction

Nowadays, with the increase in the demand for hydrocarbon resources found on the seabed, the use of parallel multiple pipelines for transporting oil, gas, and their derivations to refineries and end-users has become common. For the reasons such as economic analysis, risk reduction, and ensuring the continuity of fluid transfer during a periodic maintenance, installing two or more subsea pipelines is mainly preferred to a single pipeline. Additionally, many pipe-laying barges are capable of simultaneously deploying two pipelines. Regular monitoring conducted on the seabed of subsea pipelines indicates the formation of numerous scour holes along their length, leading to the creation of free spans. The gradual expansion of these free spans along the pipeline results in a significant increase in oscillatory loads, causing fatigue and the eventual rupture of the pipeline. Over the past few decades, numerous studies have been conducted on scour beneath single subsea pipelines caused by unidirectional flow, waves, and their combination (flow-wave interaction).

Research on local scour under pipelines has primarily been approached in two ways: (1) using physical models and laboratory tests, and (2) employing numerical models to solve mathematical equations related to flow dynamic and sediment transport.

In the past, a number of researchers, namely Kjeldsen et al., Leeuwestein, Bijker, Ibrahim, and Nalluri investigated local scour around a single pipeline under the influence of unidirectional flow in the clear water and live bed conditions[1]. They concluded that the depth of scour caused by the flow was proportional to the pipe diameter, flow velocity, depth of flow, and the size of sediment particles.In a series of laboratory experiments on scour around subsea pipelines, Mao [1] discovered that the scour process comprises two distinct phases: tunnel scour in the initial stages and lee wake scour in the later stages of scour development [1]. Vanbeek analyzed the depth of scour beneath pipelines induced by a constant current [2]. Chiew introduced an empirical function linking the gap flow through the scour hole to the prevailing flow conditions [3]. The authors formulated empirical equations for prediction of the maximum scour depth beneath subsea pipelines. Sumer and Fredsøe extensively investigated scour initiation, the characteristics of equilibrium scour profiles, and the variables that impact them [1]. Furthermore, Cheng et al. performed an experimental study to explore local scour beneath a rigid pipeline. The scour was caused solely by waves and combined wave-current actions [4].

Then, Chao and Hennessy, Chiew, Li and Cheng [5], Hosseini et al. [6], and Sumer et al. [7] developed numerical models based on the potential flow theory to estimate scour profiles. Further, the numerical models that can describe accurately turbulent flows have been employed by Brørs [8], Li and Cheng , Liang et al., Fuhrman et al. [9], and Larsen et al. [10] to simulate the scour process. Also, Yeganeh et al. proposed a two-phase model to explore tunnel erosion beneath submarine pipelines subjected to unidirectional flow [11]. However, despite the possibility of pipelines being placed in a parallel setup, most research on local scour beneath subsea pipelines has predominantly focused on a single, isolated pipeline.

Several studies have been conducted to examine the scouring process beneath two parallel pipelines. Westerhorstmann et al. [12] investigated the impact of a gap (G) between tandem pipelines and found that when G/D=0.5, the scour depths beneath the two pipelines were smaller than those where G/D=1. Moreover, under combined wave and current flow conditions, the scour depths were reduced compared to those observed under steady current flows. Zhang et al. [13] conducted experiments on local scour beneath two identical pipelines arranged in tandem, considering various gap ratios under both live bed and clear water conditions. For clear water conditions, it was observed that when G/D<2, the equilibrium scour depth beneath the upstream pipeline was greater than that of the scour beneath the downstream pipeline, a trend that differs from what is seen in live bed conditions. Zhao et al. [14] explored the effect of the gap ratio between two pipelines on scour through extensive numerical simulations, with gap ratios ranging from 0.5 to 5. Their findings indicated that placing the two pipelines as close as possible would minimize scour depths under both clear water and live bed conditions. Zhao et al. also employed numerical methods to analyze the influence of gap ratio and the KC number on scour depth beneath the pipelines across a wide range of parameters. Li et al. [15] developed a 2D numerical model to study local scour beneath two tandem submarine pipelines under combined wave and current conditions.

Dan et al. employed the CFD–DEM method to simulate local scour around two tandem pipelines [16]. Their findings showed that when G/D≤2, the equilibrium scour depth beneath the upstream pipeline is slightly greater than thatwas under the downstream pipeline. Recently, Maddah et al. conducted an experimental research on scouring around submarine pipelines grouped together due to steady currents [17]. The authors found that while the width of the scour hole increased over time, the scour depth beneath both the downstream and upstream pipes was less than the maximum scour depth observed beneath a single pipe. As previously mentioned, several studies have focused on investigating into the scour phenomenon beneath two tandem pipelines under steady flow, with only one study examining the combined effects of wave and current. Nevertheless, this study presents a specialized investigation of the impact of tidal currents on scouring around tandem pipelines.

Tidal fluctuations continuously alter water levels in open seas, and the persistent and forceful currents produced by tides in bays, straits, and estuaries necessitate the study of phenomena associated with sediment transport, seabed level changes, and scouring around the structures situated in these areas. The behavior of the tide can be considered as a gravity wave that causes periodic changes in the sea level and flow direction. Also, the tidal current is a mostly horizontal bidirectional current that is the result of a tide.

In the Persian Gulf and the Strait of Hormuz, as well as its estuaries, there are multiple pipelines laid down on the sea bed. Significant local scours have been observed during surveys of these submarine pipelines in service. In those areas due to the continuity and dominance of currents caused by tides, it is necessary to investigate the phenomena related to scouring around the subsea parallel pipelines to be illuminated better than before.

More recently, Hosseini et al. [18] simulated scour below a single pipeline resulting from bidirectional currents using FLOW3D. In their numerical model application, they specifically focused on the flow characteristics in the Persian Gulf. Then, they utilized an experimental model to study the clear-water current conditions, taking into account parameters likes velocity, depth, and the number of tidal cycles required to reach the equilibrium stage. Thus, this research study aims to both experimentally and numerically investigate the scouring process around two submarine pipelines in tandem due to tidal currents and compare the results with those obtained under steady currents for clear-water conditions.

Figure 1 depicts a schematic diagram illustrating the scouring beneath two tandem pipelines of equal diameter. The diameter of the pipeline and the distance between them are represented as D and G, respectively. Pipelines 1 and 2 refer to the upstream and downstream pipelines, respectively. The scour depth beneath the center lines of pipelines 1 and 2 are denoted as S_1 and S_2, respectively.

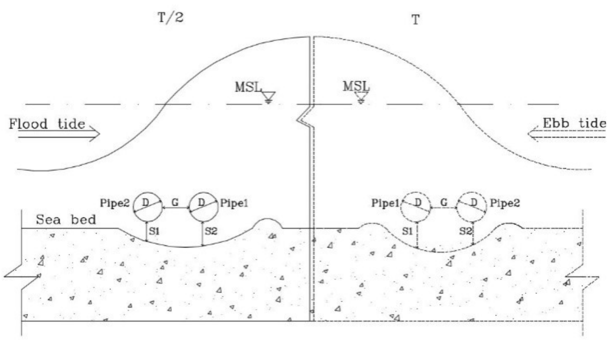

Figure 1. Sketch of scour below two pipelines due to tidal current.

2. Dimensional analysis

The equilibrium scour depth around a pipeline relies on (a) Hydraulic characteristics, (b) Physical properties of the fluid, (c) Geometric parameters, and (4) Sediment parameters. The parameters can be summarized as follows:

$S = f\,(g, \rho, \nu, U, h, T, D, G_{,50}, \sigma_g, \rho_s, B)$ (1)

Here, it may be assumed that the influence of viscosity and sediment non-uniformity are disregarded [19]. Also, using the Buckingham Pi theorem, Eq. (1) can be condensed and expressed as follows:

$S/D = f\,(Fr, KC, Re, \theta, G/D)$ (2)

On the other hand Sumer and Fredsøe[20]found that the scour depth had a weak correlation with the pipeline's Reynolds number. Consequently, Eq. (2) was simplified as follows:

$S/D = f\,(Fr, KC, \theta, G/D)$ (3)

Then, the resultant equation indicates that the non-dimensional scour depth generally depends on the Froude number, the KC number, the Shields parameter (i.e., θ), and the relative gap between pipes.

3. Materials and methods

Figure 2 displays the experimental setup and dimensions of the flume. A bidirectional flume was constructed for this study at Hydraulics Research Laboratory of Sahand University of Technology. Its length, width and depth are 10m, 0.6m and 1m respectively. Two wired gates are positioned at each end of the flume, allowing control over the water depth. A pump is located beneath the right end of the flume, supplying water from tanks to the channel.The flow direction, velocity, and depth are precisely controlled and regulated using side valves and valves adjacent to the pump.

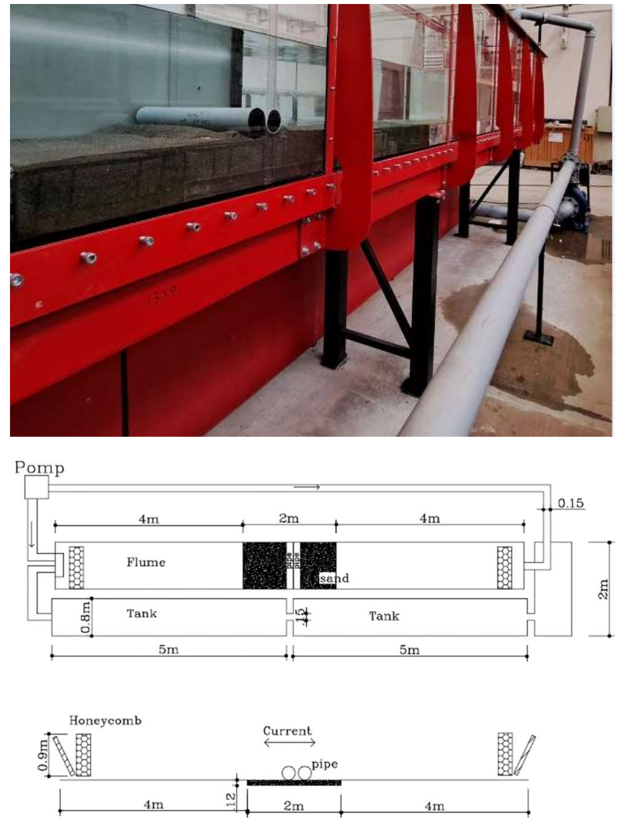

Figure 2: Experimental flume and Sketch of the tests set up.

4. Sediment properties and threshold of movement

The sediment properties used in this study are identical to those that have been used in Asrari et al [19].

For this study, two methods have been employed to ascertain the velocity equivalent to the threshold of movement, which are as follows:

First, sediment movement has been evaluated using the modified Shields diagram [20], based on the dimensionless shear stress parameter θ=0.031. Then, the average critical velocity value is determined using the Melville formula [21]:

$$\frac{U_c}{U_f} = 5.57\log(5.53\frac{h}{d_{50}}) \quad (4)$$

Here, *Uc* is the critical mean approach flow velocity for sediments movement and U_f signifies the frictional velocity on the bed. The sediments materials used for this research have a median diameter d_{50}=0.78 mm and h is flow depth.

$$\theta = \frac{U_f^2}{g(s-1)d_{50}} \quad (5)$$

Finally, the critical flow velocity corresponding to the threshold of movement (U_c) is calculated to be 35 cm/s.

In the experimental procedure, once sediment grains began to move, a water velocity meter was deployed to precisely measure the flow speed. The averaged recorded flow velocity was 32.3 cm/s. Therefore, with $U \leq U_c$, the dominance of clear water conditions is evident.

5. Model scale

In coastal modeling, inertia and gravity forces typically dominate, making it crucial to accurately scale the Froude number. The Froude number can significantly impact the scour process, as it affects the water surface profile and, consequently, the flow field around the pipeline. The studied area of this research is the striate of Hormuz in Persian Gulf. The tidal pattern along the Persian Gulf's near shore regions follows a semi-daily rhythm, with a period of approximately 12 hours. In this region, several submarine pipelines have been constructed and are currently operational. The physical model used for this study is a 1:30 scaled-down model of a main gas pipeline. Consequently, the corresponding parameters of the model, based on the measured parameters of the region, have been determined using the Froude law [22].Then, the tidal model periods corresponding to semi-daily (12 hours) is 2.2 hours and water depth is 25-30 cm. In addition, diameter of modeled pipe was 6 cm.

6. Simulation of tidal currents

A simplified approximation of tidal flow involves periodically reversing the direction of a flow with a constant depth-averaged velocity [21 and 22].To scale the flow velocities, the maximum peak velocity within the selected tidal signal has been matched to the flow intensities necessary to achieve clear-water conditions ($U_{<}U_c$), considering the specific sediment properties involved. Figure 3 displays the time history of bidirectional currents velocities for the semi-daily tide. Then, a simplified symmetrical tidal signal was utilized in the laboratory. Each half cycle was divided into five time steps: two during acceleration, one at the peak, and two during deceleration, with a constant current velocity maintained at each time step.

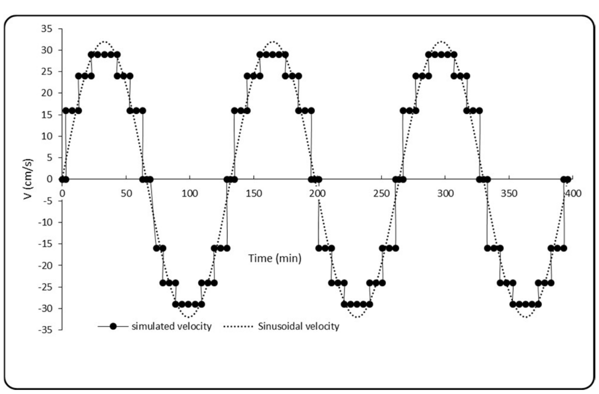

Figure 3: Time history of simulated tidal current velocity

7. Tests program

For examining the scouring caused by tidal flow beneath tandem pipelines with G/D =0.1 and comparing it with the scouring resulting from steady currents, two groups of experiments were conducted under both bidirectional and steady currents in clear water conditions. The first group (A) investigated bidirectional currents. The second one (B) concentrated on studying local scour beneath the pipelines exposed to steady currents. A summary of the experimental set and results are shown in Table 1.

Table 1: A summary of the scour tests conditions.

	Test No.	Cycles	G/D	h (cm)	S_1/D	S_2/D
A	TT1	3	0	25	0.33	0.32
	TT2	3	0	30	0.23	0.23
	TOT3	3	1	25	0.25	0.19
	TOT4	3	1	30	0.21	0.16
B	UTT5	-	0	25	0.36	0.29
	UTT6	-	0	30	0.27	0.23
	UTOT7	-	1	25	0.31	0.21
	UTOT8	-	1	30	0.23	0.13
	U9	-	∞	25	0.48	-
	U10	-	∞	30	0.37	-

8. Experimental results and discussion

The significant results will be analyzed to identify the underlying causes and to compare scour beneath tandem pipelines under both tidal and steady currents. Figures 4, present camera images depicting scour profiles at different time intervals for test no. TT1.

Based on the experimental results, the mechanism of the scouring process in the case of tandem pipes can be explained as follows: the initiation of scour is primarily associated with seepage flow within the bed. In the case of tandem pipes, the elongation of the flow path within the bed causes a delay in piping and subsequent scouring compared to a single pipe. When the pipes are closely positioned, they function nearly as a unified entity, resulting in simultaneous scouring beneath them, resembling the behavior observed with a single pipe. For the first half cycle under steady current conditions, the scour hole initially formed beneath the upstream pipe and then extended to underneath of the downstream pipe. Then, during the initial stages of scouring, the scour depth below the upstream pipe exceeded than that of the downstream pipe. However, over time, this difference decreased, and eventually, the scour depth below the downstream pipe became greater than that of the upstream pipe. Simultaneously, a sand dune is gradually formed downstream. In the second half cycle, however, when the flow direction changed, the above process is reversed and the scour profile becomes more symmetrical. This scenario continued in subsequent cycles until reaching to the equilibrium stage. It is worth noting that, in this scenario, the base of the scour hole exhibits a wider dimension compared to that of a single pipe.

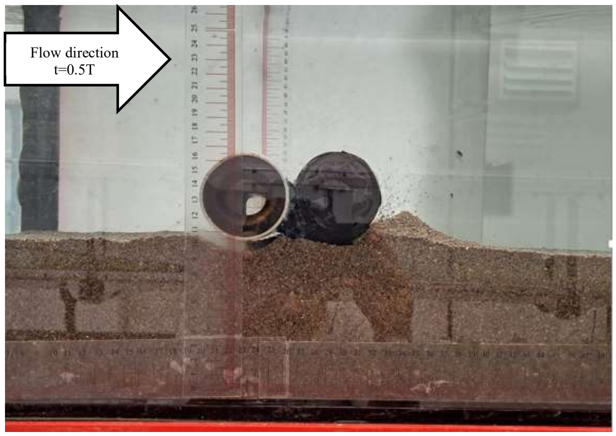

a: Firth half period (t=0.5 T)

b: Sixth half period (t=3 T)

Figure 4: Scouring profile at the end of the first half cycle and the sixth half cycle for tandem pipes, semi daily tidal currents

From the figures 4, it is evident that the second pipe creates a sheltering effect. This effect eliminates the formation of vortices, thereby reducing lee wake erosion and resulting in a narrower scour hole compared to that of a single pipe.

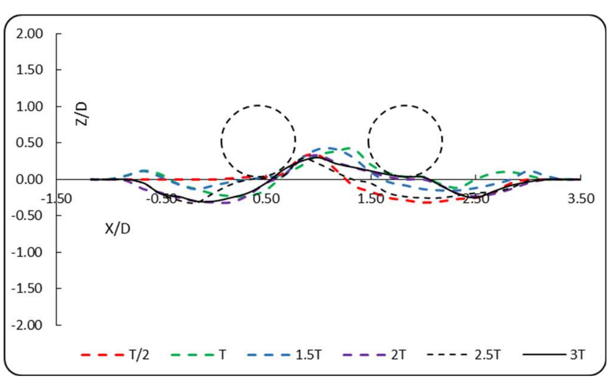

Figure 5: Scouring profile in six consecutive half-cycles of tidal flow (test no. TOT3)

When the G/D=1, the scouring pattern becomes more intricate (figure 5). In the first half cycle, during the flood direction from right to left, sediments removed from underneath of the first pipe (right one) accumulate near the second pipe (left one). Additionally, when the flow direction reverses during the ebb, sediments discharged from the second pipe partially fill the scour hole formed beneath the first pipe. This process continues in alternating cycles.

Figure 6 presents a comparison of the bed scouring profiles for parallel pipes under bidirectional flow conditions. Then, the profile of tandem pipes with G/D approximately equals to zero is contrasted with the scouring bed profile of parallel pipes under steady flow conditions. It is evident that the scour depth under steady flow exceeds the scour depth caused by bidirectional flow. Furthermore, when the G/D=1, the scouring depth is less compared to the cases where the pipes are placed closely together. In this scenario, each pipe forms a distinct scour hole with limited dimensions.

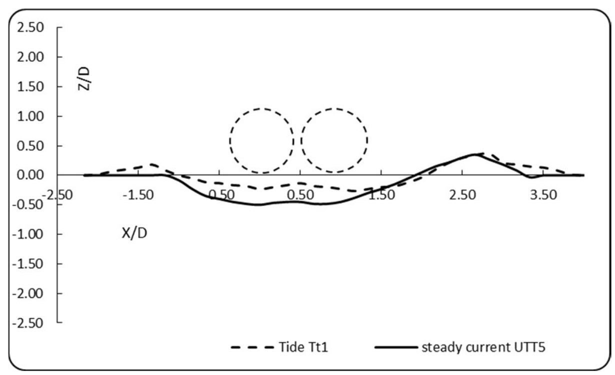

Figure 6: Bed profile under two tandem pipes due to the steady and tidal currents

Therefore, it may be concluded that for the case of two parallel pipelines, the flow dynamics and its interaction with the mobile bed exhibit greater complexity compared to a single pipeline. Depending on the gap between the two pipelines, the lee wake vortices generated by the upstream pipeline are carried downstream and may interact with the downstream pipeline, influencing its scour depth.

9. Numerical model

For this section, a numerical model application is presented using the Flow3D (v11.1) software. The model simulates various stages of the scour process caused by tidal flow beneath the single and parallel pipelines. These stages include the onset of scour, tunnel erosion, lee-wake erosion and scour development using sediment transport equations. The input data include flow velocities, water depth, pipe diameter, and sediment characteristics. The outputs are flow field around the pipe (velocity, pressure) as well as the depth and width of the scour profile at the end of each tidal cycle. The scour phenomenon is a process that stems from the interaction between the pipeline, the erodible seabed, and the flow field. Therefore, analyzing such a phenomenon requires an understanding of two sets of equations: hydrodynamic equations and sediment transport equations. The hydrodynamic equations must be solved at first stage of every time step since sediment transport equations depend on the flow velocity components. Also, for the scour phenomenon, due to the existing a turbulent flow and vortices around the structure, turbulence models must be employed for numerical simulation.

10. Hydrodynamic Equations

The proposed numerical framework solves the incompressible unsteady Reynolds-averaged Navier-Stokes (URANS) equations utilizing the k-ε turbulence model [8]. The governing equations for the flow in Cartesian coordinate system include a continuity equation and fluid momentum equations:

$$\frac{\partial u_i}{\partial x_i} = 0 \tag{7}$$

$$\frac{\partial u_i}{\partial t} + u_j \frac{\partial u_i}{\partial x_j} = -\frac{1}{\rho_f}\frac{\partial p}{\partial x_i} + \tag{8}$$

$$\upsilon \frac{\partial}{\partial x_j}\left(\frac{\partial u_i}{\partial x_j} + \frac{\partial u_j}{\partial x_i}\right) - \frac{\partial \overline{u_i' u_j'}}{\partial x_j} + \left(\frac{\rho_s}{\rho_f} - 1\right) cg\,\delta_{i3}$$

In the above equations, u_i represents the velocity components along the coordinate axes x_i, p is the pressure, and ρ is the fluid (water) density.

$$\overline{u_i' u_j'} = \upsilon_T\left(\frac{\partial u_i}{\partial x_j} + \frac{\partial u_j}{\partial x_i}\right) - \frac{2}{3}\delta_{ij} k \tag{9}$$

$$k = \frac{1}{2}\overline{u_k' u_k'} \tag{10}$$

To close the system of equations, the k–ε model is deployed for this model application. Then, the model includes two additional equations: one for k (turbulent kinetic energy) and the other for ε (rate of dissipation of turbulent energy).

$$\frac{\partial k}{\partial t} + u_j \frac{\partial k}{\partial x_j} = -\frac{\partial}{\partial x_j}\left(\frac{\upsilon_T}{\sigma_c}\cdot\frac{\partial k}{\partial x_j}\right) + P + G - \varepsilon \tag{11}$$

$$\frac{\partial \varepsilon}{\partial t} + u_j \frac{\partial \varepsilon}{\partial x_j} = -\frac{\partial}{\partial x_j}\left(\frac{\upsilon_T}{\sigma_c}\cdot\frac{\partial \varepsilon}{\partial x_j}\right) \tag{12}$$

$$+ \left(C_{\varepsilon 1} P - C_{\varepsilon 2} P + C_{\varepsilon 3} \max\ (0, G)\right)\frac{\varepsilon}{k} \tag{13}$$

$$\upsilon_T = \frac{C_\mu k^2}{\varepsilon}$$

In these equations, ν_T is the turbulent eddy viscosity, and k represents the turbulent kinetic energy. P is the production rate of turbulent kinetic energy k by shear velocity, and G is the production rate of k by gravity, defined as:

$$P = \upsilon_T \frac{\partial u_i}{\partial x_j}\left(\frac{\partial u_i}{\partial x_j} + \frac{\partial u_j}{\partial x_i}\right) \tag{14}$$

$$G = \left(\frac{\rho_s}{\rho_f'} - 1\right) cg \frac{\upsilon_T}{\sigma_c}\frac{\partial c}{\partial x_3} \tag{15}$$

11. Sediment model

Utilizing a sediment model, researchers simulate the phenomenon of local scour beneath the pipeline. This model predicts sediment movement by estimating sediment erosion, advection, and deposition. The processes of entrainment, deposition, bed-load transport, and suspended load transport collectively define the process of sediment transport. Entrainment and deposition are described as conflicting processes regulating the overall exchange rate between settled and suspended sediments. When the bed shear stress surpasses the critical shear stress, grains on the seabed may be dislodged and become suspended.

11.1. Suspended load transport

The suspended load is determined by solving a turbulent-diffusion equation that is derived from the concentration continuity principle [23]

$$\frac{\partial c}{\partial t} + \left(u_j - w_s \delta_{j3}\right)\frac{\partial c}{\partial x_j} = -\frac{\partial \overline{c' u_j'}}{\partial x_j} \tag{16}$$

11.2. Bed load transport

The sediment transport rate as bed-load per unit width (considering the bed stability parameter θ and the median sediment grain diameter, d_{50}) is determined using the Nielsen equation as follows:

$$q_0 = 12\sqrt{g\left(\rho_s/\rho - 1\right)d^3}\left(\theta - \theta_{cr}\right)\theta^{\frac{1}{2}} \tag{17}$$

The importance of using the Nielsen model lies in the fact that the results obtained from the numerical model show good agreement with experimental results. Furthermore, the numerical model converges in a shorter amount of time.

12. Boundary condition

-At the inlet and outlet boundaries, the conditions of specific velocity and outflow are applied periodically during successive half-cycles. Moreover, at the boundaries of both the inlet and outlet, the water elevations are held constant, assuming a hydrostatic pressure distribution.

-A symmetry boundary condition has been applied to the water surface

-For the sides (walls) and the channel be (Ymin, Ymax, and Zmin), solid boundaries were implemented as the boundary conditions. To evaluate the impact of these boundaries on flow, a widely recognized empirical equation for the standard wall function is employed (Zhao et al., 2015).

$$\frac{U}{u_*} = \frac{1}{\mathcal{K}} \ln\left(\frac{30y}{k_s}\right) \quad (18)$$

Where k_s is the bed roughness, $\mathcal{K}$ is the von Karman constant and equals to 0.4 and y is the distance from the wall [19].

-No-slip boundary conditions are applied at the pipelines surfaces, indicating that the velocities at these boundaries are zero.

13. Numerical method

The FLOW3D software was used for the section of numerical simulation of this study. The Volume of Fluid (VOF) technique is employed to monitor free water surface. Further, the model incorporates the Fractional Area/Volume Obstacle Representation (FAVOR) approach to model the intricate geometric regions within fixed rectangular meshes.

In Flow-3D, a basic grid consisting of rectangular elements was utilized, offering the benefits of regularity to enhance numerical accuracy and ease of generation. Consequently, a series of simulations were performed using various mesh sizes, focusing on both the accuracy of the numerical solution and the quality of the input data. Prior to commencing any numerical analyses, it is imperative to carefully select an appropriate mesh size. The mesh size should be determined such that it adequately captures all the intricate details of the phenomenon being analyzed. During this discretization process, the dimensions of the channel (i.e., length, width, and depth) are considered to be 200, 60 and 30 cm in the x, y, and z directions, respectively. The finest mesh resolution surrounding the pipe is approximately 6 mm, ensuring that the value of y+ closely approximates 65 during computation. It is noted that a y+ value ranging from 30 to 100 is deemed suitable for the turbulence model.

14. Model validation

In this section, the numerical evaluations have been conducted using two methods to ensure the accuracy of the results. First, to validate the hydrodynamics of the numerical model, a comparison was made with the experimental results of Omrani et al. [23], see figure 7. Based on their findings, which were obtained for the flow separation around a pipe with a diameter of 6cm, the length of the downstream vortex was calculated to be 45 centimeters. For the current study, the vortex length was found to be 46.2 cm, showing good agreement between the numerical results of the present research and the experimental results.

In the second stage, the numerical results of scour development were compared with experimental results. For this purpose, the depth of scour obtained from the numerical model of a single pipe under steady flow was compared with two sets of results provided by previous published data (Table 2).

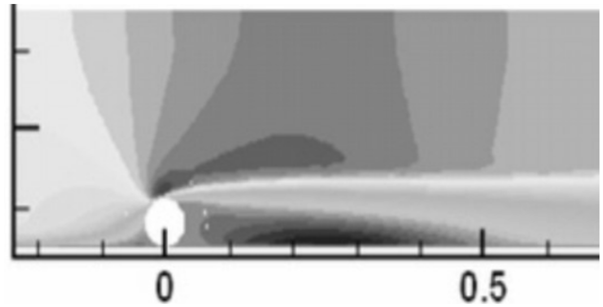

(7a):

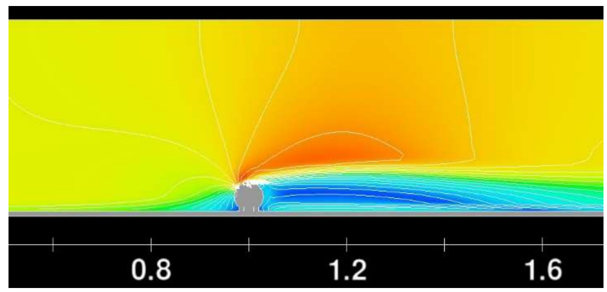

(7b):

Figure 7: Flow filed around pipe, a: Omrani et al. and b: this study.

It can be seen from table2 that the results of present numerical model compared to the results obtained from previous published data are in good agreements.

Table 2: Verification of the present numerical results for a single pipe.

Reference	Model type	D (cm)	S/D
Hosseine et al. [18]	Experimental	6	0.39
Asrari et al [26]	Numerical	6	0.42
This study	Numerical	6	0.43

15. Model applicable

The primary objective of this study is to explore the phenomenon of local scour and the factors that influence on it around two parallel pipelines. As indicated in table 2, the specific parameters are as follows: The diameter of the pipeline is D = 6 cm. The lengths of the sediment beds at the upstream and downstream are 15D, with the latter having a significant impact on the results of the numerical analyses. Furthermore, the flow depth equals to 5D and the depth of the sediment bed is equal to 10 cm. As mentioned in section 1, Hosseini et al. [18] conducted a number of simulations on the scour beneath pipelines arising from bidirectional currents using FLOW3D. The aim here is to juxtapose the results of the numerical simulations with those of the experimental study. To achieve this, the sediment characteristics and pipe diameter remain consistent in both methodologies. The Shields parameter θ is equal to 0.031 for both the experiment and simulation presented herein. This alignment, according to Larsen et al. [10], is acceptable as a non-dimensional comparison between the numerical simulation and the experiment. The comparison is done in terms of S/D over the non-dimensional time T*, expressed as:

$$T^* = \frac{\sqrt{g(s-1)d_{50}^3}}{D^2}t \qquad (19)$$

Where t is the physical time. It can be ensured that the non-dimensional scour developments are comparable between two different scales once the Shields parameter is kept the same.

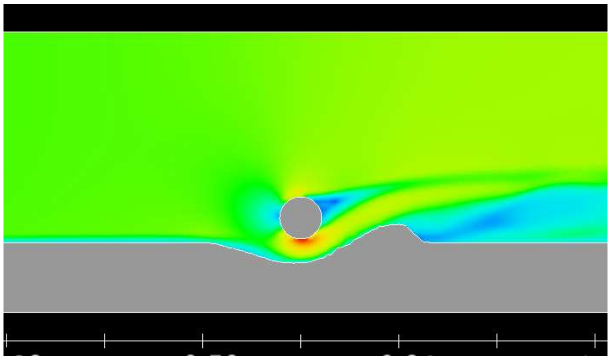

(8a) Single pipe

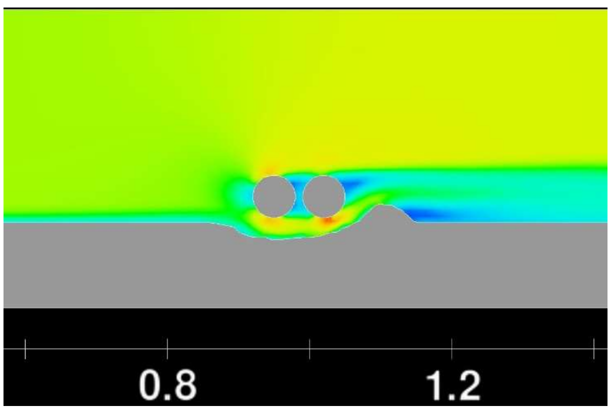

(8b)Tandem pipes G/D=0.1

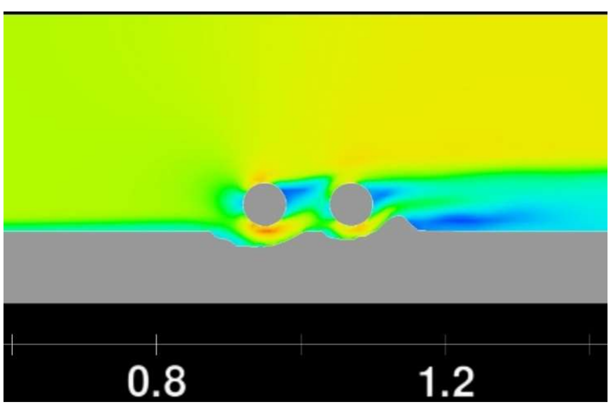

(8c)Tandem pipes G/D=1

Figure 8: Equilibrium scour profile beneath single pipe (a) and tandem pipes with (G/D=0.1 , 1) (b and c) due to steady current(T^*=14.4) .

In Figures 8, the equilibrium steady current-induced scour profiles for single and two parallel pipes with G/D= 0.1, 1 are compared (T*=14.4). As seen, the equilibrium scour depth for the single pipe is greater than that of the tandem pipelines.

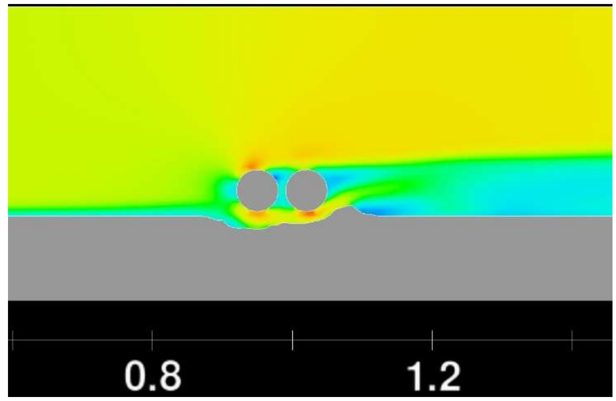

(9a) t=T/2

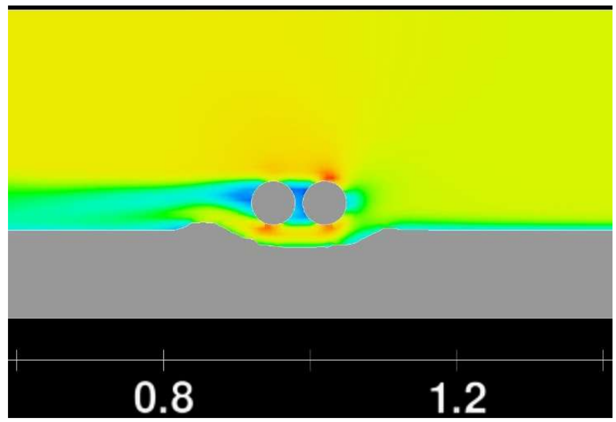

(9b) t=T

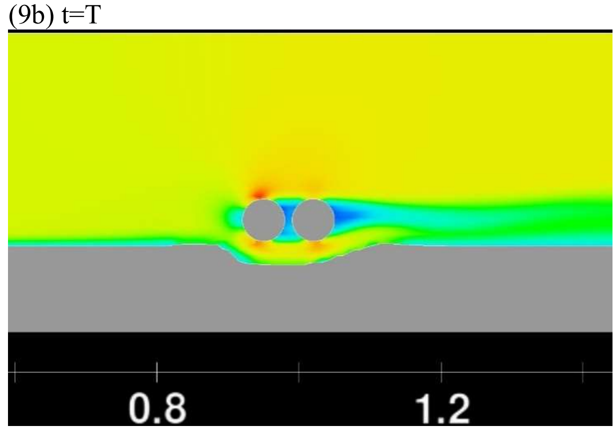

(9c) t=2.5T

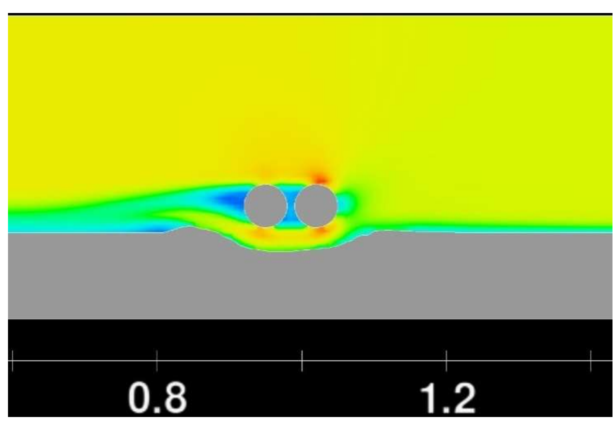

(d) t=3T

Figures 9: Scour profile change with time, calculated by the numerical model

Also under clear water conditions, it becomes evident that for $0 < G/D \leq 1$, the equilibrium scour depth of the upstream pipeline surpasses that of the downstream pipeline. In additions, the bed profiles of the sandy bed across three cycles for G=0.1, and $U/U_c = 0.9$, are depicted in figures 9.

As can be seen during the initial half cycle, the depth of the scour hole escalates rapidly over time. By the conclusion of the first half cycle, two scour holes appear beneath the pipes, with S_1 being larger than S_2 ($S_1 > S_2$), and a sandy dune forms downstream of pipe 2 (Figure 9a). In the subsequent half cycle, as the flow direction reverses, the scour hole beneath pipe2 gradually deeper. Meanwhile, S_1 decreases and another sandy dune arises behind pipe 1 concurrently, as shown in Figure 9b. For the third and fourth half cycles, the variations in the scour depth become notably small, but the width of scouring profile expands, leading to an enlargement of the scouring hole area. This phenomenon indicates the dominance of vortices throwing in the transverse progress of the scour profile, with the reversal of flow direction further intensifying the effect of eddies at this stage, resulting in an equilibrium scour profile with an almost symmetrical shape by the end of the sixth half cycle.

Finally, in table 3 the relative scour depths beneath two tandem pipelines, obtained from experimental data and numerical results for the tidal and unidirectional currents compared with each other.

Table 3: Comparison of the experimental data and numerical results

		Numrical model		Experimental model	
Flow regim	**G/D**	**S1/D**	**S2/D**	**S1/D**	**S2/D**
	0	0.38	0.38	0.35	0.35
Tidal current	1	0.24	0.22	0.27	0.25
	0	0.36	0.24	0.35	0.3
Steady current	1	0.37	0.22	0.33	0.23

As shown in table 3, there are some discrepancies between the two sets of results. However, the numerical results are relatively close to the experimental data and the maximum error is about 10%. The differences between the numerical results and the experimental data may partly be due to the reduced channel length in the computational domain, mesh size, the turbulence model and the bed load formula used in the numerical simulation. Further, some errors may occur in the experimental measurements.

16. Conclusions

This investigation examines the local scouring surrounding two parallel pipelines, scrutinized the phenomenon through the experimental and numerical investigations under clear water conditions with varying gap ratios. The key conclusions drawn include:

1. Unlike to the steady currents, for G/D<1, tidal currents result in a scour profile with two dunes at the upstream and downstream of the pipelines. The shape of the scour hole is nearly symmetrical and the slope is gentler in both directions.
2. In steady currents, as the distance between the two pipes increases from G/D= 0 to 1, the width of the scour hole expands. Also the scour depth decreases with increasing the G/D.
3. In tidal currents for G/D=1 by reversing direction of the flow in each half cycle, the scour hole under the second pipeline is periodically filled by the sediment removed beneath the upstream pipeline. Therefore it is an engineering achievement for scour protection of subsea multiple pipelines.
4. The scour depths beneath the pipelines exhibit a strong positive dependence on the magnitude of flow velocity and G/D. However, no scour is observed below the downstream pipeline when the flow velocity is smaller than $0.6U_c$.
5. The progression of the scour bed profile reveals through three distinct stages: the initiation of scour, scour development, and scour stabilization. During the onset of scour, a sand bar arises between the pipelines, with the size and position of the bar being linked to the initial velocity and G/D. Throughout the scour development, sediment particles transport is the most intense beneath the pipelines.
6. Across all scenarios (G/D = 0 - 1), the scour depth beneath both the downstream and upstream pipes remains lower than the maximum scour depth underneath the single pipeline.
7. For tandem pipelines, the scour depth under uniform flow conditions surpasses that induced by bidirectional flow. Moreover, when the gap between pipes equals the diameter of the pipe, the scour depth is lower compared to the pipes that are placed in close proximity to one another. In such instances, each pipe exhibits a distinct scour hole with constrained dimensions.

17. Acknowledgment

The authors express their gratitude to Dr. Reza Ghiassi, Associate Professor of Civil Engineering Faculty at the University of Tehran, for eagerly consulting the first author.

List of Symbols

B	channel width
d_{50}	median size of bed sediments
D	pipe diameter
Fr	Froude number
g	gravitational acceleration
G	distance between pipes
h	water depth
k	bed roughness
KC	Keulegan-Carpenter number
q_0	sediment transport rate as bed-load per unit width
Re	Reynolds number
s	specific gravity of the sediment

S	scour depth
t	time
T	tidal period
T^*	dimensionless time scale
u_f	frictional velocity on the bed
U_c	critical approach flow velocity
x; y	coordinates in stream-wise and lateral direction
z	vertical direction
θ	shields parameter
θ_{cr}	critical shields parameter
ρ	water density
ρ_s	density of sediment
ν	kinematic viscosity
σ_g	the geometric standard deviation of sediments

18. References

[1]Sumer B. M., Fredsøe J., (2002), The mechanics of scour in the marine environment. World Scientific, Vol. 17, pp 5-136. https://doi.org/10.1142/4942

[2] Vanbeek F.A., and Wind H.G., (1990), Numerical modelling of erosion and sedimentation around offshore pipelines. Coastal Eng. J., 14 pp 107-128. https://doi.org/10.1016/0378-3839(90)90013-M

[3] Chiew, Y.M., (1991). Prediction of maximum scour depth at submarine pipelines. J. Hydraulic Eng., 117(4), pp 452-466. https://doi.org/10.1061/(ASCE)0733-9429(1991)117:4(452)

[4] Cheng, N. S., Wei, M., Xu, P., Mao, R., (2020). Length scale for evaluating wave-induced pipeline scour. Ocean Eng. J., Vol. 218, 108153. https://doi.org/10.1016/j.oceaneng.2020.108153

[5]Li F., Cheng L., (1999), Numerical model for local scour under pipeline. J. Hydraul. Eng., Vol. 125, No. 4, pp 400-406. doi:10.1061/(ASCE)0733-9429(1999)125:4(400)

[6] Hosseini D., Hakimzadeh H., Ghiassi R., (2005), Numerical and Experimental Modeling of Scour around a Submarine Pipeline due to Currents. Proceedings of the Pipeline Division Specialty Conference, Houston, Texas, pp. 793-802.

[7] B.M. Sumer (2007) "Mathematical modelling of scour" Journal of Hydraulic Research Vol. 45, No. 6, pp. 723–735. doi:10.1080/00221686.2007.9521811

[8] Brors, B. (1999). Numerical modeling of flow and scour at pipelines. J. Hydraul. Eng., Vol. 125, No. 5, pp 511-525. https://doi.org/10.1061/(ASCE)0733-9429(1999)125:5(511)

[9] Fuhrman, D.R., Baykal, C., Sumer, B.M., Jacobsen, N.G., Fredsøe, J., 2014. Numerical simulation of wave-induced scour and backfilling processes beneath submarine pipelines. Coast Eng. 94, 10–22.https://doi.org/10.1016/j.coastaleng.2014.08.009

[10] Larsen, B.E., Fuhrman, D.R., Sumer, B.M., 2016. Simulation of wave-plus-current scourbeneath submarine pipelines. J. Waterway. Port, Coastal, and Ocean Engineering, 142(5), Article04016003.https://doi.org/10.1061/(ASCE)WW.1943-5460.0000338.

[11] Yeganeh-Bakhtiarya, A., Kazeminezhad M. H., Etemad-Shahidi, A., Baas J. H. , Cheng, L., (2016). Euler–Euler two-phase flow simulation of tunnel erosion beneath marine pipelines. Applied Ocean Research 33 (2011) 137–146.https://doi.org/10.1016/j.apor.2011.01.001

[12] Westerhorstmann, J.H., Machemehl, J.L., Jo, C.H., 1992. Effect of pipe spacing on marinepipeline scour. Proceeding Of The 2nd International Offshore and Polar Engineering Conference. San Francisco, June 14–19.

[13] Zhang, Q., Draper, S., Cheng, L., Zhao, M., An, H., 2017. Experimental study of localscour beneath two tandem pipelines in steady current. Coast Eng. J. 59, 1750002.DOI: 10.1142/S0578563417500024.

[14] Zhao, M., Vaidya, S., Zhang, Q., Cheng, L., 2015. Local scour around two pipelines in tandem in steady current. Coast Eng. 98, 1–15.http://dx.doi.org/10.1016/j.coastaleng.2015.01.001.

[15]Li A., Ong M., C., Fuhrman D. R., Larsen B. L., (2020).Numerical investigation of wave-plus-current induced scour beneath twosubmarine pipelines in tandem. Coastal Engineering 156 (2020) 103619. https://doi.org/10.1016/j.coastaleng.2019.103619.

[16] Dan H., Wen T., Liang S., Fen L., Xiangying J., Zheng D., (2019). Numerical simulation of local scour around two pipelines in tandem using CFD–DEM method.Applied Ocean Research 93 (2019) 101968.https://doi.org/10.1016/j.apor.2019.101968.

[17] Maddah S., Kolahdouzan F., Eftekhari A., Singh V. P., Afzalimehr H., (2021).Experimental investigation of scouring in groups of parallel pipelines. International Journal of Hydraulic Engineering 2021, 10(2): 27-34. DOI: 10.5923/j.ijhe.20211002.01.

[18] Hosseini D., Hakimzadeh H., Ghiassi R., (2023), Simulation of scour beneath a pipeline due to tidal currents. J. Marine Eng., Vol. 19, No. 39, pp. 1-11.doi: 10.61186/marineeng.19.39.1.

[19] Asrari, S., Hakimzadeh, H. and Kardan, N. (2021), Investigation on the local scour beneath piggyback pipelines under clear-water conditions. China Ocean Eng. J., Vol 35, No. 3, pp. 422-431. https://doi.org/10.1007/s13344-021-0039-7

[20] Van Rijn L. C., (2005). Principles of sedimentation and erosion engineering in rivers, estuaries and coastal seas. Aqua Publications.
[21] Schendela A., Hildebrandta A., Gosebergb N., Schlurmann T., (2018), Processes and evolution of scour around a monopile induced by tidal currents. Coastal Eng. J., Vol. 139, pp. 65–84.doi.org/10.1016/j.coastaleng.2018.05.004.
[22] Porter K. E., Simons R., Harris J. and Ferradosa T. F., (2012), Scour development in complex sediment beds., 33rd Coastal Eng. proceedings, Vol. 1, No. 33, Santander, Spain.
[23] Omrani S. and Hakimzadeh H., (2009). Numerical and experimental investigation of flow separation phenomenon around smi-buried pipelines due to steady currents" Journal of marine Eng.,Vol. 4, No. 8, pp 65-76. https://doi.org/ 20.1001.1.17357608.1387.4.8.6.5